



HAL
open science

Chromium site selective substitution in $\text{Ca}_3\text{Co}_2\text{O}_6$: Influence on the magnetic properties of an ising-like triangular lattice

Delphine Flahaut, A. Maignan, S. Hebert, Christine Martin, R. Retoux, V.
Hardy

► **To cite this version:**

Delphine Flahaut, A. Maignan, S. Hebert, Christine Martin, R. Retoux, et al.. Chromium site selective substitution in $\text{Ca}_3\text{Co}_2\text{O}_6$: Influence on the magnetic properties of an ising-like triangular lattice. *Physical Review B: Condensed Matter and Materials Physics (1998-2015)*, 2004, 70 (9), pp.094418–1–094418–8. 10.1103/PhysRevB.70.094418 . hal-01499385

HAL Id: hal-01499385

<https://hal.science/hal-01499385>

Submitted on 19 Jan 2022

HAL is a multi-disciplinary open access archive for the deposit and dissemination of scientific research documents, whether they are published or not. The documents may come from teaching and research institutions in France or abroad, or from public or private research centers.

L'archive ouverte pluridisciplinaire **HAL**, est destinée au dépôt et à la diffusion de documents scientifiques de niveau recherche, publiés ou non, émanant des établissements d'enseignement et de recherche français ou étrangers, des laboratoires publics ou privés.

Chromium site selective substitution in $\text{Ca}_3\text{Co}_2\text{O}_6$: Influence on the magnetic properties of an Ising-like triangular lattice

D. Flahaut, A. Maignan,* S. Hébert, C. Martin, R. Retoux, and V. Hardy

Laboratoire CRISMAT, UMR CNRS ISMR 6508, 6 bd Maréchal Juin, 14050 CAEN Cedex 4, France

(Received 18 December 2003; published 23 September 2004)

The structure of the $\text{Ca}_3\text{Co}_2\text{O}_6$ compound is made of chains on a triangular array. The intra- and interchain coupling are ferromagnetic and antiferromagnetic, respectively, and the chain itself contains a 1:1 alternation of CoO_6 trigonal prisms (TP) and octahedra (oct.). The Co^{3+} spin states are high spin ($S=2$) and low spin ($S=0$) in the TP and the oct., respectively. It is found that a few percent of Cr^{3+} ($S=3/2$) substituted for the low spin $\text{Co}_{\text{oct}}^{3+}$ ($S=0$) greatly affect the magnetic properties. Both coupling constants of the antiferromagnetic (interchain) and ferromagnetic (intrachain) interactions decrease as x increases up to $x=0.10$ in $\text{Ca}_3\text{Co}_{2-x}\text{Cr}_x\text{O}_6$. This is reflected by the decrease of the magnetization saturation and of the magnetic field characteristic of the ferri- to ferromagnetic transition, below the Néel temperature. These results are interpreted on the basis of an antiferromagnetic coupling between $\text{Co}_{\text{oct}}^{3+}$ and its high spin $\text{Co}_{\text{TP}}^{3+}$ neighbours. Furthermore, the magnetization jumps, observed below $T < 10$ K, tend to be suppressed on the isothermal magnetization curves as soon as $x=0.05$. These results emphasize the great sensitivity of the $\text{Ca}_3\text{Co}_2\text{O}_6$ magnetic behavior to the presence of a magnetic foreign cation, with, in particular, a T_N decrease probed by specific-heat measurements.

DOI: 10.1103/PhysRevB.70.094418

PACS number(s): 75.10.Pq, 75.30.Cr, 75.30.Hx, 75.60.Ej

I. INTRODUCTION

The richness of the physical properties of the cobaltites is related to the ability of cobalt cations to adopt not only several oxidation states but also several spin states. This is well known in the case of the perovskite LaCoO_3 for which the trivalent cobalt exhibits spin state transitions as a function of temperature, the low spin (LS) state being stabilized at low T which leads to a zero magnetic susceptibility.¹ More recently, the physical properties of the one-dimensional compound $\text{Ca}_3\text{Co}_2\text{O}_6$, another compound containing trivalent cobalt, have been shown to exhibit several original features.²⁻⁵ The structure of this cobaltite, derived from the K_4CdCl_6 rhombohedral structure,² consists of chains set on a triangular lattice (see inset of Fig. 2). Interestingly, the chains are made of two types of polyhedron, trigonal prisms (TP) and octahedra (oct.), alternating along the chain and sharing triangular faces. These chains are separated by the calcium cations, and the Co-Co interchain distance (5.24 Å) is longer than the cobalt-cobalt intrachain distance (2.59 Å). It should be noted that this intrachain distance is much shorter than the Co-Co distance in the perovskite (~ 3.8 Å). The original behavior of $\text{Ca}_3\text{Co}_2\text{O}_6$ comes from the ability of Co^{3+} to adopt several coordinations, by adapting its spin state, illustrated at low temperature by its high spin and low spin states in the prism and octahedron, respectively.³ It results in an antiferromagnetic and ferromagnetic interchain and intrachain coupling, respectively, with a very large magnetic anisotropy ($D \sim -25$ K)⁴ giving to spins a strong Ising-like character. This was referred to as Ising chains on a triangular lattice in several references (see for instance Ref. 5). Among the original electronic and magnetic properties of $\text{Ca}_3\text{Co}_2\text{O}_6$, the existence of a first magnetization plateau together with an abrupt transition at about 3.6 T on the magnetic field driven magnetization (M) curve is probably one of the most remark-

able feature reflecting the close energies of the ferri- ($M = 1/3 \times M_{\text{saturation}}$) and ferromagnetic ($M = M_{\text{saturation}}$) configurations.²⁻⁵ Such a transition was predicted theoretically for the case of Ising magnetic moments on the triangular lattice.⁶ In the first studies of the $\text{Ca}_3\text{Co}_2\text{O}_6$, magnetic properties performed on single crystals and on magnetically aligned powder,^{4,5} by applying the magnetic field and measuring the magnetization along the cobalt chains, several additional M plateaus were also found at low T ($T \ll T_N$) by both static [superconducting quantum interference device (SQUID) magnetometer] and dynamic [vibrating-sample magnetometer (VSM)] M measurements. Note that this is in contradiction with the recent claim that such additional plateaus could be observed only with a VSM.⁷

It was initially proposed that the existence of several M steps on the $M(H)$ curves could be due to the close energy of different arrangements of the cobalt magnetic moments in the triangular plane perpendicular to the chains.⁵ Alternatively, starting from the observation that the additional M steps, at low T , appear at fixed intervals of magnetic fields ($H_{\text{steps}} = n \times 1.2$ T where n is an integer such as $n \leq 6$), an analogy to the quantum tunneling of molecular magnets has been made.⁸ In the latter, the field driven magnetization curves of magnetic clusters (Mn_{12} , Fe_8 , etc. ...), at low enough temperatures, exhibit regularly spaced magnetization steps corresponding to tunneling of the magnetization of the so-formed macrospins.⁹⁻¹¹ The comparison to other magnetic Ca_3CoMO_6 phases [$M = \text{Ir}^{4+}$,¹² Rh^{4+} (Ref. 13)] shows that the additional M features observed in $\text{Ca}_3\text{Co}_2\text{O}_6$ are not found when the cobalt cation sitting in the octahedron is replaced by an other cation.

In order to test the sensitivity of the M jump to the substitution at the Co^{3+} octahedral site, chromium has been retained. Such substitution can give also information on the origin of the intrachain ferromagnetic coupling in $\text{Ca}_3\text{Co}_2\text{O}_6$.

The choice of Cr^{3+} was motivated by previous reports on the existence of $\text{Sr}_3\text{LnCrO}_6$ (Ref. 14) phases where the chromium cation is trivalent and sits in the octahedron, and also, by the fact that the presence of the high spin (HS) Cr^{3+} magnetic moments ($t_{2g}^3, S=3/2$) instead of $S=0$ for LS $\text{Co}_{\text{oct}}^{3+}$ is expected to disturb the intra- and interchain coupling. Note also that one could have also selected a nonmagnetic (d^0 or d^{10}) trivalent cation but the substitution of LS($S=0$) $\text{Co}_{\text{oct}}^{3+}$ cation by another ($S=0$) trivalent cation may not affect so rapidly the magnetic properties. In this case, the larger amounts of substituting cations which would be required to perform the study may lead to a chemical problem linked to the solubility limit. In this respect, it must be emphasized that the site controlled substitution is not trivial and one must be very cautious when speaking of $\text{Ca}_3\text{Co}_{2-x}\text{M}_x\text{O}_6$ compounds, where M is a foreign metal, and that the combination of different techniques for structural characterizations are most of the time necessary to confirm the composition of those phases. In the following, we report on the magnetic properties of $\text{Ca}_3\text{Co}_{2-x}\text{Cr}_x\text{O}_6$ compounds with $x \leq 0.10$. It is found that small Cr^{3+} percentages strongly weaken the intrachain ferromagnetic coupling. Furthermore, only 5% of Cr^{3+} per cobalt are sufficient to suppress the regularly spaced magnetization steps exhibited by $\text{Ca}_3\text{Co}_2\text{O}_6$ in oriented powders of the $\text{Ca}_3\text{Co}_{2-x}\text{Cr}_x\text{O}_6$ cobaltites.

II. EXPERIMENTAL

Polycrystalline samples of $\text{Ca}_3\text{Co}_{2-x}\text{Cr}_x\text{O}_6$ ($x=0, 0.02, 0.05, 0.1, 0.15$) were synthesized via solid-state reactions in air. The reagents, CaO , Co_3O_4 , and Cr_2O_3 were intimately mixed and placed in alumina crucibles. The powders were calcined at 800°C for 24 h and then pressed in the form of bars under 1 ton/cm^2 and heated at 1000°C for 24 h. The sample for electron microscopy study was prepared by smoothly crushing the crystallites in alcohol. The small flakes were deposited on a holey carbon film, supported by a copper grid. Electron diffraction and energy dispersive spectroscopy (EDS) characterizations were carried out at room temperature with a JEOL 2010 electron microscope. The samples were characterized at room temperature by using a Philips x-ray diffractometer using $\text{CuK}\alpha$ (from 10 to 100° in 2θ with steps of 0.02°). Lattice parameters and cell volumes were obtained from the Rietveld method using the FULLPROF program.

The alternative magnetic susceptibilities of $\text{Ca}_3\text{Co}_{2-x}\text{Cr}_x\text{O}_6$ ($x=0, 0.02, 0.05, 0.1$) were measured using a quantum design ac-dc magnetometer within an ac magnetic field of 10 Oe and frequencies from 10^2 to 10^4 Hz. Magnetization measurements were performed with magnetometers (extraction method) working with a maximum field of 5 or 9 T. All the magnetic field dependent magnetization measurements were made by using “aligned” samples prepared as follows: a mixture of $\text{Ca}_3\text{Co}_{2-x}\text{Cr}_x\text{O}_6$ ($x=0, 0.02, 0.05, 0.1$) powder and grease (in the 1:7 mass ratio) has been submitted to a 9 T field at 320 K and then cooled down to 150 K keeping the field constant. At this stage, the field was finally removed, and subsequent magnetization at lower T were made. Due to the presence of grease, measurements are

limited to low temperature so that all the temperature dependent magnetic measurements have been made on unaligned pieces of the as-prepared ceramic bars. Specific heat measurements have been performed for pieces of ceramic samples for $\text{Ca}_3\text{Co}_2\text{O}_6$ ($x=0.00$) and $\text{Ca}_3\text{Co}_{1.9}\text{Cr}_{0.1}\text{O}_6$ ($x=0.10$). Details of the measurement technique are described elsewhere.¹⁵

III. RESULTS

A. Structural characterizations

Structure refinements of $\text{Ca}_3\text{Co}_{2-x}\text{Cr}_x\text{O}_6$ ($x=0, 0.02, 0.05, 0.1, 0.15$) were carried out in the R-3c space group ($N^\circ 167$). As shown in Fig. 1, the lattice parameters increase roughly linearly with the chromium content up to $x=0.10$. For higher chromium contents ($x=0.15$), small extra peaks can be detected on the x-ray diffraction pattern and, concomitantly, the values of the structural parameters tend to saturate. So, chromium cation can be substituted for cobalt in $\text{Ca}_3\text{Co}_2\text{O}_6$ but its content is limited to $\sim 5\%$ of chromium per cobalt. Thus, the study of the magnetic properties has been limited to the samples corresponding to $x \leq 0.10$. The EDS and electron diffraction investigation of about 15 crystallites of the limit compound $\text{Ca}_3\text{Co}_{1.9}\text{Cr}_{0.1}\text{O}_6$ sample showed no deviation from the nominal cationic composition. The average cation content is $\text{Ca}_{3.03 \pm 0.08}\text{Co}_{1.87 \pm 0.06}\text{Cr}_{0.10 \pm 0.08}$. According to Shannon’s ionic radii values,¹⁶ because of the very close radii of HS Cr^{3+} and HS Co^{3+} , 0.615 and 0.61 Å, respectively, the substitution of HS Cr^{3+} for HS Co^{3+} in the trigonal prism could not account for the increase of the cell parameters. The HS Cr^{3+} in the prism might induce a LS to HS transition of the surrounding Co^{3+} in the octahedron, which could also be responsible for the increase of the cell parameters. However, as shown in Ref. 17, such a spin transition is not favored due to the smaller covalency of the Cr—O bond compared to the Co—O one (i.e., the electronegativity of Cr^{3+} is smaller than the one of Co^{3+} , 1.66 and 1.8, respectively¹⁸). In contrast, the substitution in the octahedron of HS Cr^{3+} (0.61 Å) for LS Co^{3+} (0.545 Å) must induce a unit cell expansion as the Cr^{3+} content increases. Furthermore, this preferential occupation of the octahedron for the Cr^{3+} is consistent with the report that, in the $\text{Sr}_3\text{LnCrO}_6$ compounds (Ln=lanthanide),

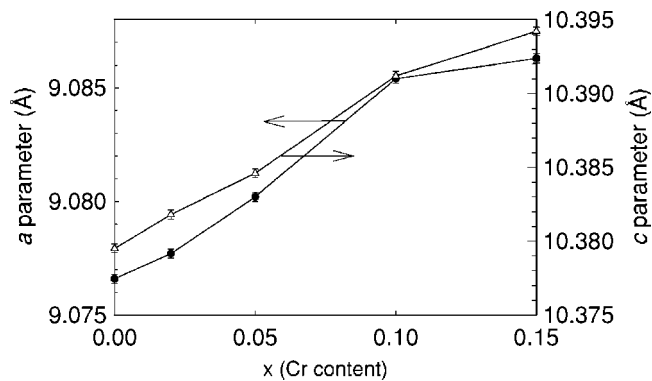


FIG. 1. Evolution of the lattice parameters versus chromium content.

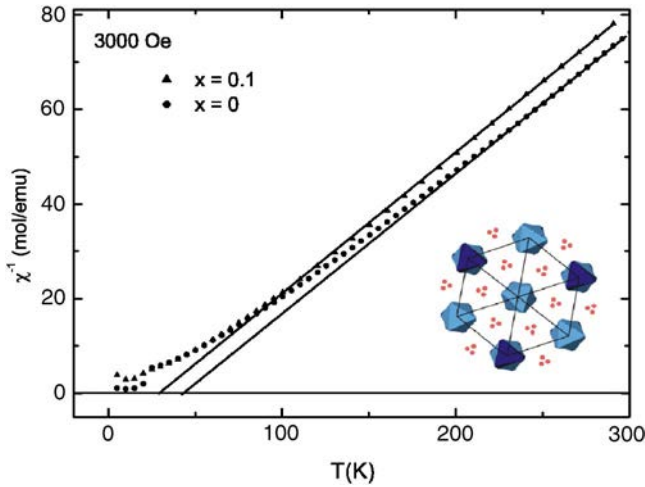


FIG. 2. T dependence of the inverse of the magnetic susceptibility for $x=0.02$ and 0.10 . The Curie-Weiss fitting curves are shown by straight lines. Inset: Projection on the hexagonal ab plane of the $\text{Ca}_3\text{Co}_2\text{O}_6$ structure showing the triangular arrangement of the chains.

the Ln^{3+} and Cr^{3+} cations sit in the TP and oct., respectively.¹⁴ Also previous reports by Kageyama *et al.* on the HS Fe^{3+} substitution in $\text{Ca}_3\text{Co}_2\text{O}_6$ (Ref. 19) have shown that when the substituting cation is in the TP, the moment of Fe^{3+} behave as isolated paramagnetic moments. Fe^{3+} is not exchange-coupled to LS Co^{3+} . However, as shown in the following, our magnetic data show that Cr^{3+} is strongly coupled with the Co^{3+} . So this different magnetic behavior is another proof that the Cr^{3+} do not sit in the TP but rather in the octahedron.

B. Magnetic susceptibility

In the series $\text{Ca}_3\text{Co}_{2-x}\text{Cr}_x\text{O}_6$, the occupation of an octahedron by a trivalent $t_{2g}^3 e_g^0$ ($S=3/2$) cation creates some defects of alternating ($S=2$)/($S=3/2$)/($S=2$) magnetic moments in the ferromagnetic ($S=2$)/($S=0$)/($S=2$) chains of $\text{Ca}_3\text{Co}_2\text{O}_6$. As shown in Fig. 2 on the T dependent inverse magnetic susceptibility curves (unaligned samples), the θ_p values decrease as x increases, reaching $\theta_p=32$ K for $x=0.10$ against $\theta_p=40$ K for $x=0.00$. Thus, the ferromagnetic intrachain interaction is reduced in comparison with $\text{Ca}_3\text{Co}_2\text{O}_6$ and contrasts with the θ_p increase induced by iridium, reaching $\theta_p=150$ K for $\text{Ca}_3\text{CoIrO}_6$ in which Co^{2+} and Ir^{4+} are ferromagnetically coupled.¹² This result may indicate that the Cr^{3+} magnetic moments are antiferromagnetically coupled to their ($S=2$) Co^{3+} neighbors.

The study of the magnetic properties, at low temperature, confirms that the Cr-substitution modifies the magnetic behavior of $\text{Ca}_3\text{Co}_2\text{O}_6$. This can be seen on the field-cooling (fc) or zero-field-cooling (zfc) $\chi(T)$ curves collected with a field of 0.3 T (Fig. 3). Starting from the high temperature side of the zfc $\chi(T)$ curve, as T decreases, one first observes for $\text{Ca}_3\text{Co}_2\text{O}_6$ a χ rise below about 25 K which corresponds to T_N .³ Second, χ exhibits a maximum at about 10 K, T below which χ_{zfc} drops (Fig. 3). Comparing these curves to

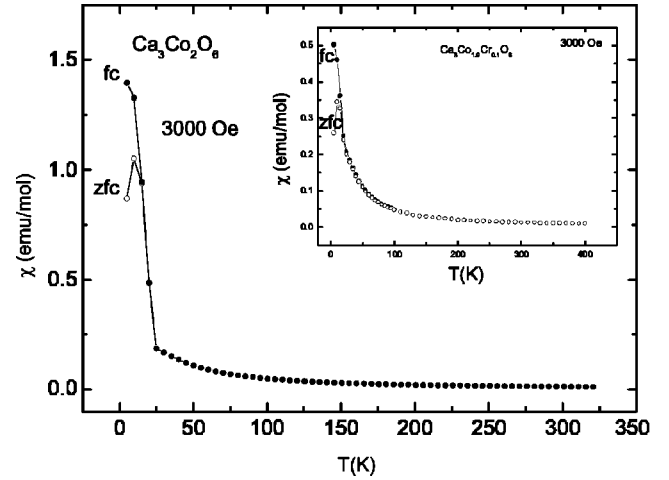
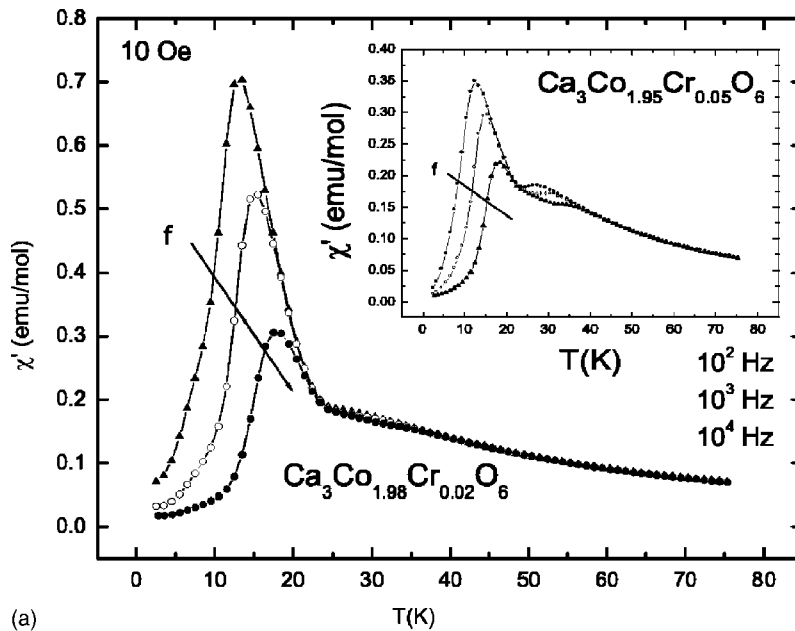


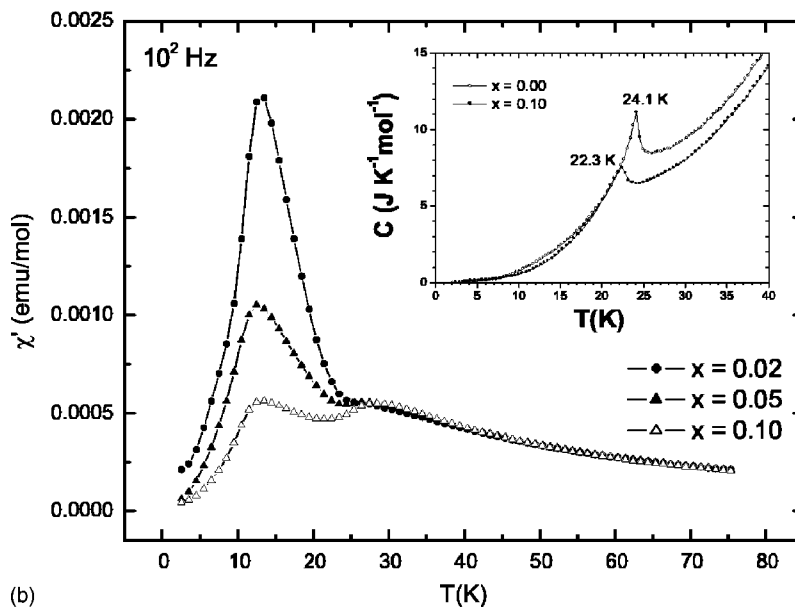
FIG. 3. T dependence of the magnetic susceptibility χ . The data are deduced from M data collected upon warming in zero-field-cooling (zfc) and field-cooling (fc) modes. The magnetic field values are indicated on the graph.

those obtained for $\text{Ca}_3\text{Co}_{1.9}\text{Cr}_{0.1}\text{O}_6$ (inset of Fig. 3), one can clearly see that both χ rise below T_N and χ maximum are affected by the Cr^{3+} substitution (Fig. 3).

These features are more clearly observed on the curves of ac- χ magnetic susceptibility [$x=0.02$ and $x=0.05$ in Fig. 4(a)] which have been performed by using several frequencies in the range 10^2 to 10^4 Hz. By combining the curves collected for the different samples at 10^2 Hz [Fig. 4(b)], a clear decrease of χ' maximum value, χ'_{\max} , is found. Since the χ' rise below T_N is connected to the intrachain ferromagnetic coupling, which starts to develop below T_N , one can conclude that the intrachain coupling is strongly sensitive to the Cr^{3+} substitution. Furthermore, from the enlargement of these $\chi'(T)$ curves in the T_N region, it can also be observed that a second χ' maximum develops in the 25 – 30 K T region and becomes clearer as the Cr^{3+} content increases. In order to probe the effect of the Cr^{3+} substitution on T_N , specific-heat measurements have been made for $\text{Ca}_3\text{Co}_2\text{O}_6$ ($x=0.00$) and $\text{Ca}_3\text{Co}_{1.9}\text{Cr}_{0.1}\text{O}_6$ ($x=0.10$). The results given as an inset of Fig. 4(b) show that each $C(T)$ curve exhibits a peak characteristic of the setting of antiferromagnetism¹⁵ at $T_N=24.1$ K. and $T_N=22.3$ K for $x=0.00$ and $x=0.10$, respectively. Thus, the Cr^{3+} substitution also weakens the antiferromagnetism. Consequently, the second χ maximum in the 25 – 30 K T range in Fig. 4(b) is not related to T_N but most probably reflects the presence of an underlying broad χ' maximum beyond T_N as also observed in $\text{Ca}_3\text{CoRhO}_6$ (Ref. 15) and $\text{Sr}_3\text{NiIrO}_6$.²⁰ Such a maximum could reflect the existence of one-dimensional magnetic correlations (see for instance Ref. 21). As for the undoped $\text{Ca}_3\text{Co}_2\text{O}_6$ compound, the $\chi'(T)$ curves depend on the frequency (f) of the ac excitation magnetic field [Fig. 4(a)]. Using an analogy with the spin glass (SG), a freezing temperature T_f corresponding to χ'_{\max} can be defined. This effect of f on T_f can be quantified by the parameter K , $K=\Delta T_f/(T_f^* \Delta \log 2\pi f)$.²² We obtain $K=0.15$ for $x=0.00$, $K=0.17$ for $x=0.02$, and $K=0.26$ for $x=0.05$. Those values are very large in comparison to K



(a)



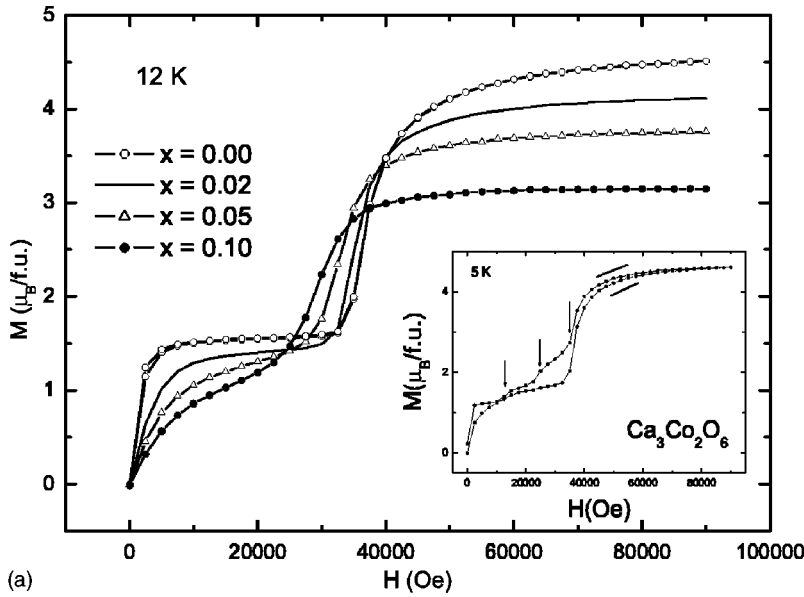
(b)

$\approx 10^{-2}$ in typical SG²² but are consistent with that reported in $\text{Ca}_3\text{CoRhO}_6$, $K=0.10$.²³ All those K values are more typical of superparamagnet⁵ than SG and they reflect the very slow dynamics of the spins in this class of compounds. In that respect, the K increase with x shows that the spins become slower in the time window of the experiments. In addition to this effect at T_f , the second χ' maximum in the T region of 25–30 K, is found to also be frequency dependent as shown for $x=0.05$ in the inset of Fig. 4(a). If this second χ' maximum is linked to one-dimensional magnetic correlations, this f dependent behavior could also be the result of a very slow dynamic of the spins in the chains existing even without long-range ordering. Finally, it must be emphasized that the χ' values for the lowest T of the measurements, $T=2.5$ K, decrease as the Cr^{3+} content increases, to reach $\chi' \sim 0$ when $f=10^2$ Hz for the samples such as $x > 0.02$ [Fig. 4(a)].

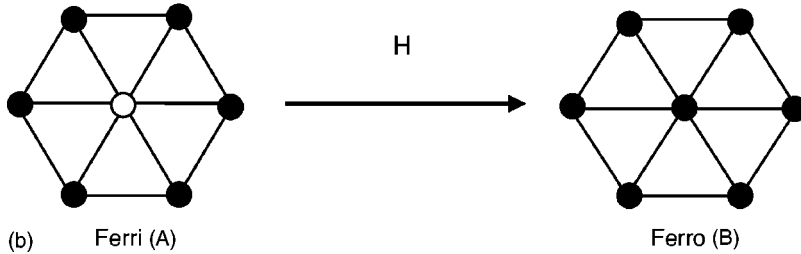
FIG. 4. (a) AC magnetic susceptibility (χ') as a function of T for $x=0.02$ and $x=0.05$ (inset). The frequency values are indicated (b) AC magnetic susceptibility χ' as a function of T for $\text{Ca}_3\text{Co}_{2-x}\text{Cr}_x\text{O}_6$ ($x=0.02, 0.05, 0.10$) for $f=10^2$ Hz. Inset: Temperature dependence of the specific heat under zero field for $x=0.00$ (open circles) and $x=0.10$ (closed circles).

C. Field dependent magnetization

To try to overcome the noncomplete alignment of the chains magnetization with the magnetic field direction in ceramic samples, all measurements of the magnetization versus magnetic field have been realized on aligned samples using the method described in the experimental part. In the case of $\text{Ca}_3\text{Co}_2\text{O}_6$, for $T < 20$ K, the $M(H)$ curve is characterized by a first M plateau at $1/3$ of M saturation, followed by an abrupt M jump at 3.6 T which corresponds to the ferri- to ferromagnetic transition [Fig. 5(a)]. In this ferrimagnetic state, on each triangle made of three ferromagnetic chains, two chains are antiferromagnetically coupled so that the magnetization value reaches only $1/3$ of the saturation magnetization [Fig. 5(b)]. This plateau is clearly evidenced on the $M(H)$ curves collected for the $x=0$ and 0.02 samples and it becomes less well defined for $x \geq 0.05$ [Fig. 5(a)]. How-



(a)



(b)

ever, the magnetic field values, necessary to induce the ferri-to ferromagnetic (Fi-Fo) transition, decrease as the chromium content increases. This is shown on the $M(H)$ curves recorded at 12 K [Fig. 5(a)] where the characteristic field $H_{\text{Fi-Fo}}$ decreases from 3.6 T down to 2.8 T for $x=0.00$ to $x=0.10$, respectively. These characteristic magnetic fields are the same on the field increasing and decreasing branches. The decrease of $H_{\text{Fi-Fo}}$ indicates that the ferrimagnetic configuration becomes less stable at the benefit of the ferromagnetic phase as the Cr^{3+} content increases. Additionally, we can also see that the saturation magnetization decreases as the Cr^{3+} content increases. This can be explained by considering the structural data. From the latter, the Cr^{3+} magnetic cations enter at the octahedral site (nonmagnetic in the pristine compound) so that a decrease of the saturation magnetization can be induced if the magnetic moments of Cr^{3+} are antiferromagnetically coupled to their HS $\text{Co}_{\text{TF}}^{3+}$ neighbors and thus break the intrachain ferromagnetic coupling between Co^{3+} . It should also be emphasized that, due to the χ decrease induced by the Cr^{3+} substitution, as x increases the $1/3$ magnetization plateau becomes less well-defined, requiring a larger magnetic field to be reached consistently with the decrease of the dM/dH slope in the low field region.

One additional feature on the $M(H)$ curves of $\text{Ca}_3\text{Co}_2\text{O}_6$ is the existence of extra magnetization steps appearing as T becomes lower than 10 K as shown in the inset of Fig. 5(a) for $T=5$ K. The corresponding M jumps appear at regularly spaced values of the magnetic field ($H_{\text{steps}} \sim n \times 1.2$ T). It should be noticed that these steps are more easily detected on the magnetic field decreasing branch rather than on the in-

FIG. 5. (a) Magnetic field dependence of $M(H)$ curves collected at 12 K for $\text{Ca}_3\text{Co}_{2-x}\text{Cr}_x\text{O}_6$ ($x=0.00, 0.02, 0.05, 0.10$). Inset: $M(H)_{5\text{ K}}$ for $\text{Ca}_3\text{Co}_2\text{O}_6$. The arrows indicate the different magnetization jumps. (b) Magnetic sublattice in triangular Ising lattice, the magnetic moments are perpendicular to the triangles plane (A) ferrimagnetic and (B) ferromagnetic structure. (The closed circles represent the spin up and the open circles the down one.)

creasing branches [see Fig. 5(a)]. Although for measurements performed on crystals with a VSM, six steps can be resolved on the $M(H)$ curve collected at 2 K,⁸ one can easily observe that, with a SQUID magnetometer, the steps at $H_{\text{steps}} > 3.6$ T ($n > 3$) are hardly detectable (Fig. 6). This difference is ascribed to the effects of the magnetic field sweep rate which are out of the scope of this paper and will be discussed in a separate paper. Nonetheless, one can see that the M steps (except the M jump at 3.6 T) are sensitive to the chromium substitution since they tend to disappear as the Cr^{3+} content increases, but, at 2 K, for $x=0.05$ one step is still detectable at ~ 2.4 T, i.e., the characteristic magnetic field has not been modified by the Cr^{3+} substitution (Fig. 6).

IV. DISCUSSION

All the present results obtained by magnetic measurements point toward the strong efficiency of Cr^{3+} to disturb the magnetic behavior of $\text{Ca}_3\text{Co}_2\text{O}_6$ when substituted for Co^{3+} . The first result deals with the selectivity of the substitution with HS Cr^{3+} substituting LS Co^{3+} sitting in the octahedra. However, as shown by the structural data, the solubility range of Cr^{3+} is limited to about 10% occupation of the octahedral site. This underlines that one must be very cautious as soon as small contents of substitutions at the cobalt site are involved. The second result, induced by the Cr^{3+} substitution, concerns the magnetic properties. The magnetic susceptibility below T_N drops very rapidly showing that the ferromagnetic intrachain coupling is very sensitive to the substitution. This can be understood if one considers that

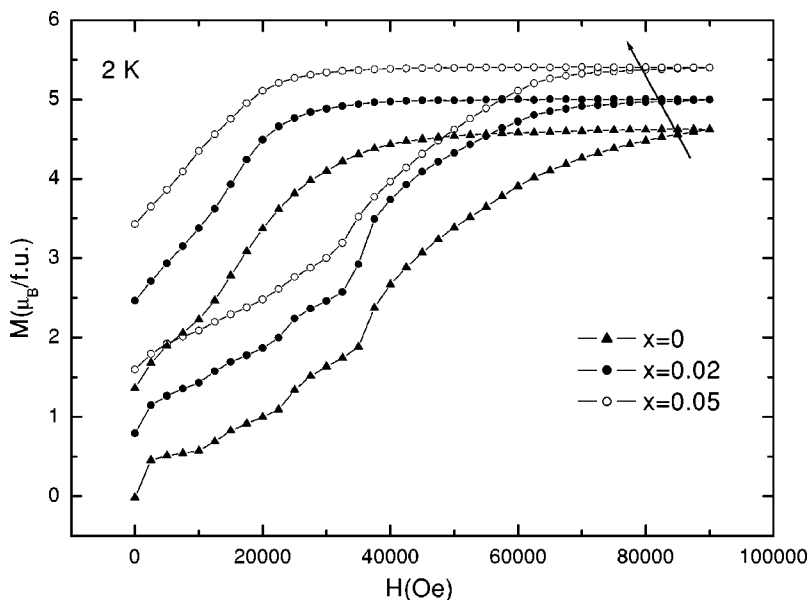


FIG. 6. $M(H)$ curves (increasing and decreasing branches) for 2 K of $\text{Ca}_3\text{Co}_{2-x}\text{Cr}_x\text{O}_6$ ($x=0.00, 0.02, 0.05$). For sake of clarity, the M values have been shifted up by $0.75 \mu_B/\text{mol}$ and $1.5 \mu_B/\text{mol}$ for $x=0.02$ and $x=0.05$, respectively.

Cr^{3+} couples antiferromagnetically to its cobalt neighbors which breaks the intrachain long range ferromagnetic coupling. The induced magnetic disordering can also be inferred from the frequency dependence of the ac magnetic susceptibility. A clear increase of frequency dependence of the freezing temperature as the Cr^{3+} content increases is induced. Simultaneously, the ac magnetic susceptibility values reach $\chi' \sim 0$ at 2.5 K as soon as $x=0.02$ in $\text{Ca}_3\text{Co}_{2-x}\text{Cr}_x\text{O}_6$. Such a zero value for χ' at low temperature was found in the case of $\text{Ca}_3\text{CoRhO}_6$ (Ref. 24) and taken as an evidence for the freezing of the partially disordered antiferromagnetic state (PDA), proposed theoretically by Mekata *et al.*⁶ The first experimental observation of the PDA state was made in the CsCoCl_3 compound which is also made of magnetic chains setting on a triangular array but with antiferromagnetic Co-Co interactions for both intra- and interchain coupling.²⁵ In the PDA state, one over the three chains belonging to a same triangle loses its magnetic coherence whereas the two remaining ones are antiferromagnetically coupled, leading to a zero net magnetization. As the sample is further cooled down the PDA state becomes “frozen” with a spin freezing along the chains responsible for a nul magnetic susceptibility. In this respect, the creation of antiferromagnetic defects along the chains induced by the Cr^{3+} substitution could make the magnetic behavior closer to the PDA state. This would explain the decrease of χ' at low T .

The last part of the study deals with the effect of the HS $\text{Co}_{\text{oct}}^{3+}$ for LS $\text{Co}_{\text{oct}}^{3+}$ substitution on the M substeps at low T . First, it is clear from the values of the saturation magnetization that the Cr^{3+} magnetic moments are not ferromagnetically coupled to their Co^{3+} , even for field up to 9 T. Second, the Cr^{3+} substitution makes decreasing the characteristic magnetic field of the ferri- to ferromagnetic transition $H_{\text{Fi-Fo}}$ from 3.6 T down to 2.8 T for $\text{Ca}_3\text{Co}_{1.9}\text{Cr}_{0.1}\text{O}_6$. In a model of Ising chains, the $H_{\text{Fi-Fo}}$ field is linked to the interchain antiferromagnetic coupling constant J' through the relation $|J'| = g\mu_B H_{\text{Fi-Fo}}/12S$. By taking $g=2$ and $S=2$, one obtains J' values varying from $J' = -0.20$ K for $x=0.00$ to $J' = -0.16$ K for $x=0.10$. The decrease of $H_{\text{Fi-Fo}}$ as the Cr^{3+}

content increases could thus be understood as a decrease of the interchain magnetic energy induced by this substitution. Finally, the fact that the substep tends to be suppressed as the Cr^{3+} content increases is difficult to discuss since the origin of such steps is still a matter of debate. Two scenarios are proposed: (i) magnetic field induced transitions between different configurations of the chain magnetization on the triangular lattice, as proposed in Ref. 5, between different PDA phases,²⁶ and (ii) quantum tunneling of the magnetization.⁸ Whatever the good scenario is, the substeps have been reported only for $\text{Ca}_3\text{Co}_2\text{O}_6$ though a large number of magnetic $\text{A}_3\text{BB}'\text{O}_6$ have been studied. This shows that the values of intra- and interchain magnetic coupling energies in $\text{Ca}_3\text{Co}_2\text{O}_6$ are “ideal” for observation of this feature. As shown by several observations, the intrachain ferromagnetic coupling weakens as more and more chromium is substituted for cobalt in $\text{Ca}_3\text{Co}_2\text{O}_6$. By using the models of Ref. 8 (see also caption of Fig. 7) to fit the high temperature part of the $\chi(T)$ curves, one can extract the intrachain ferromagnetic coupling constant J . From the experimental and fitting curves of Fig. 7, one obtains a decrease of J as the Cr^{3+} content increases. For instance, as x increases from 0 to 0.10 in $\text{Ca}_3\text{Co}_{2-x}\text{Cr}_x\text{O}_6$, J decreases from 7.8 to 4.3 K. Combining these values to those of J' , it is found that the $|J'/J|$ ratio tends to increase as the Cr^{3+} increases, $|J'/J|$ values being equal to 0.026 and 0.036 for $\text{Ca}_3\text{Co}_2\text{O}_6$ and $\text{Ca}_3\text{Co}_{1.9}\text{Cr}_{0.1}\text{O}_6$, respectively. Although, the Cr^{3+} for $\text{Co}_{\text{oct}}^{3+}$ substitution makes both the intra- and interchain magnetic coupling constants decrease, the intrachain magnetic coupling constant appears to be the most sensitive to the Cr^{3+} substitution. In this respect, the tendency for the substeps to disappear as the Cr^{3+} increases could be linked to the changes induced by the Cr^{3+} substitution in the magnetic constant coupling compared to $\text{Ca}_3\text{Co}_2\text{O}_6$. But, in a scenario based on the field-driven transition between different PDA phases, one would expect that the characteristic magnetic field values of these transitions to be sensitive to the magnetic coupling constants. The unchanged magnetic field of the first substep, 2.4 T, observed for $\text{Ca}_3\text{Co}_{1.95}\text{Cr}_{0.05}\text{O}_6$ is not compatible with this model. Most

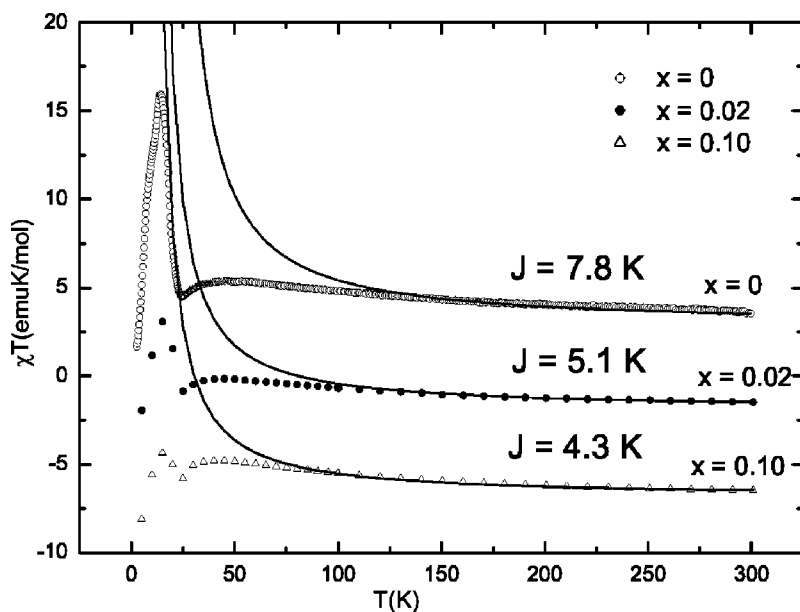


FIG. 7. χT dependence vs T . Symbols correspond to the experimental curves and solid lines to the fitting curves with the expression $\chi T = 3/4 g^2 \exp[(8J/kT)]$ from Ref. 8. The curves are fitted in the $200 \text{ K} \leq T \leq 300 \text{ K}$ range. The χT values are shifted down by subtracting 5 (emu k/mol) from curve to curve starting from $x=0.00$.

probably, the quantum tunneling of the magnetization provides a better explanation.⁸

V. CONCLUSION

The study of the series of $\text{Ca}_3\text{Co}_{2-x}\text{Cr}_x\text{O}_6$ compounds demonstrates that the solubility limit of Cr^{3+} is very limited ($x \sim 0.10$). The selectivity of the substitution at the level of the octahedra allows one to study the effect of the substitution of a magnetic cation (HS $\text{Co}_{\text{oct}}^{3+}$, $S=3/2$) for a nonmagnetic cation (LS $\text{Co}_{\text{oct}}^{3+}$, $S=0$). Remarkably, the magnetic properties are found to be very sensitive to the substitution of only small amounts of Cr^{3+} , since only 1% of chromium per cobalt ($x=0.02$) is sufficient to reduce the magnetic susceptibility below T_N . These results can be understood if one considers an antiferromagnetic coupling between Cr^{3+} and Co^{3+} . This is in agreement with the lack of ferromagnetism reported in the case of $\text{Ca}_3\text{CoMnO}_6$,²⁷ a compound for which both intra- and interchain magnetic coupling are antiferromagnetic as a result of the antiferromagnetic coupling between cobalt and manganese. At this stage one can speculate that the substitution of a nonmagnetic trivalent cation ($S=0$) for LS $\text{Co}_{\text{oct}}^{3+}$ would not have such a dramatic effect on

the magnetic properties. Subsequent studies are now in progress. In the magnetically ordered state, the presence of Cr^{3+} induces a decrease of the magnetic field value characteristic of the ferri- to ferromagnetic transition, showing a decrease of the interchain antiferromagnetic coupling constant confirmed by the T_N decrease revealed by specific heat measurements.

Finally, the magnetization substeps, observed for the lowest temperatures, are also found to be sensitive to the chromium substitution since only one substep is hardly observed for 2.5% of Cr^{3+} per cobalt but with an unchanged characteristic magnetic field. The origin of this effect is still a matter of debate.⁸

In conclusion, this study shows that a selective substitution of only small levels of impurities on $\text{Ca}_3\text{Co}_2\text{O}_6$ has a dramatic effect on the magnetic properties. This emphasizes that great care must be taken during the preparation of such samples in order to avoid spurious effects coming from off stoichiometric chemical formula. The use of selective site substitutions, i.e., in the magnetic prism or in the nonmagnetic octahedron opens possibilities to study the original magnetic properties of the very large family of the compounds crystallizing into the $\text{A}_3\text{BB}'\text{O}_6$ structure.²⁸

*Corresponding author: Fax: (+33)231951600; electronic address: antoine.maignan@ismra.fr

¹M. A. Senaris-Rodriguez and J. B. Goodenough, *J. Solid State Chem.* **118**, 323 (1995).

²H. Fjellvag, E. Gulbrandsen, S. Aasland, A. Olsen, and B. Hauback, *J. Solid State Chem.* **124**, 190 (1996).

³S. Aasland, H. Fjellvag, and B. Hauback, *Solid State Commun.* **101**, 197 (1997).

⁴H. Kageyama, K. Yoshimura, K. Kosuge, M. Azuma, M. Takano, M. Mitamura, and T. Goto, *J. Phys. Soc. Jpn.* **66**, 3996 (1997).

⁵A. Maignan, C. Michel, A. C. Masset, C. Martin, and B. Raveau, *Eur. Phys. J. B* **15**, 657 (2000).

⁶M. Mekata, *J. Phys. Soc. Jpn.* **42**, 76 (1977).

⁷S. Rayaprol, K. Sengypa, and E. V. Sampathkumaran, *cond-mat/0304426*.

⁸A. Maignan, V. Hardy, S. Hébert, M. Drillon, M. R. Lees, D. Mc K. Paul, and D. Khomskii (unpublished).

⁹D. Gatteschi, A. Caneschi, L. Pardi, and R. Sessoli, *Science* **265**, 1054 (1994).

¹⁰L. Thomas, F. Lioni, R. Ballou, D. Gatteschi, R. Sessoli, and B.

- Barbara, *Nature (London)* **383**, 145 (1996).
- ¹¹C. Sangregorio, T. Ohm, C. Paulsen, R. Sessoli, and D. Gatteschi, *Phys. Rev. Lett.* **78**, 4645 (1997).
- ¹²H. Kageyama, K. Yoshimura, and K. Kosuge, *J. Solid State Chem.* **140**, 14 (1998).
- ¹³S. Niitaka, H. Kageyama, M. Kato, K. Yoshimura, and K. Kosuge, *J. Solid State Chem.* **146**, 137 (1999).
- ¹⁴M. D. Smith and H. C. Zur Loye, *Chem. Mater.* **12**, 2404 (2000).
- ¹⁵V. Hardy, M. R. Lees, A. Maignan, S. Hébert, D. Flahaut, C. Martin, and D. Mck Paul, *J. Phys.: Condens. Matter* **15**, 5737 (2003).
- ¹⁶R. D. Shannon, *Acta Crystallogr., Sect. A: Cryst. Phys., Diffr., Theor. Gen. Crystallogr.* **A32**, 751 (1976).
- ¹⁷T. Kyômen, Y. Asaka, and M. Itoh, *Phys. Rev. B* **67**, 144424 (2003).
- ¹⁸L. Pauling, *The Nature of the Chemical Bond* (Cornell University, and Ithaca, NY, 1960).
- ¹⁹H. Kageyama, S. Kawasaki, K. Mibu, M. Takano, K. Yoshimura, and K. Kosuge, *Phys. Rev. Lett.* **79**, 3258 (1997).
- ²⁰T. N. Nguyen and H. C. Zur Loye, *J. Solid State Chem.* **117**, 300 (1995); D. Flahaut, S. Hébert, A. Maignan, V. Hardy, C. Martin, M. Hervieu, M. Costes, B. Raquet, and J. M. Broto, *Eur. Phys. J. B* **35**, 317 (2003).
- ²¹L. J. De Jongh and A. R. Miedena, *Adv. Phys.* **23**, 1 (1974).
- ²²J. A. Mydosh, *Spin Glasses* (Taylor & Francis, London, 1993).
- ²³E. V. Sampathkumaran and A. Niazi, *Phys. Rev. B* **65**, 180401 (2002).
- ²⁴S. Niitaka, K. Yoshimura, K. Kosuge, M. Nishi, and K. Katurai, *Phys. Rev. Lett.* **87**, 177202 (2001).
- ²⁵M. F. Collins and O. A. Petrenko, *Can. J. Phys.* **75**, 609 (1997).
- ²⁶T. Takagi and M. Mekata, *J. Phys. Soc. Jpn.* **64**, 4609 (1995).
- ²⁷V. G. Zubkov, G. V. Bazuey, and A. P. Tyutyunnik, *J. Solid State Chem.* **160**, 293 (2001).
- ²⁸K. E. Stitzer, J. Darriet, and H.-C. zur Loye, *Curr. Opin. Solid State Mater. Sci.* **5**, 535 (2001).